Centrifuge Testing of Model Levees atop Peaty Soil: Experimental Data

Anne Lemnitzer,[a] **A.M.EERI, Riccardo Cappa,**[a] **S.M. EERI, Samuel Yniesta** [c] **, S.M. EERI, and Scott Brandenberg,** [c] **A.M.EERI,**

Four large scale centrifuge tests were performed at the NEES@UCDavis equipment site to study the cyclic behavior of levee structures resting atop soft organic peat. The model configurations using a non-liquefiable levee focused on the seismic deformation potential of peat during primary consolidation and secondary compression. The tests performed with a sandy levee studied the liquefaction potential of saturated loose sand fill overlying soft peat as well as the levee-peat interaction under different loading conditions. The models were subjected to scaled ground motions representative of the Sacramento – San Joaquin Delta where unengineered levee fills rest atop soft compressible peat soils. System instrumentation consisted of linear potentiometers, pore pressure sensors and accelerometers. Slow data recorded at 1Hz document the settlements during spin up, application of ground motions, and spin down. Fast data sampled at 4167 Hz measured the dynamic response of the system, the excess pore pressure increase and immediate settlements. The project is archived at the NEES data repository under nees.org/warehouse/project/1161.

INTRODUCTION

This research aims to better understand the contribution of peat soil to the seismic response of levees using centrifuge models. Non-liquefiable clay levees were tested to study the post-cyclic volumetric strain behavior of the peat, and to study the deformation modes of the comparatively stiffer levee using concepts from soil-structure interaction theories. Levees composed of loose liquefiable sand were also tested to mimic a condition that characterizes some levees in the Sacramento / San Joaquin Delta, and to study the influence of the peat on the liquefaction behavior of the sand. This research will be applicable in the Delta, and in

---

[a] University of California Irvine, 4149 Engineering Gateway, Irvine, CA, 92831, USA, alemnitz@uci.edu
[b] University of California Los Angeles, 405 Hilgard Ave, Los Angeles, 90095, USA

other regions worldwide where levees rest atop peat in seismic regions (e.g., Hokkaido, Japan; Sasaki,1994), and will provide valuable experimental data to support engineering evaluation procedures for predicting levee deformations.

This paper presents experimental data from a centrifuge testing program conducted at the NEES@UCDavis equipment site from January 2013 – March 2014. Eleven preliminary small scale tests on the 1-m radius Schaevitz centrifuge helped establish the most suitable model construction techniques, which was complicated by (1) the very high compressibility of the peat material and associated geometry changes during spin-up, and (2) the need to maintain a water channel on one side of the liquefiable levee. Two investigations were then performed on the 9m-radius centrifuge at 57g, implementing lessons learned from small scale testing and preliminary analytical studies. Table 1 reports a summary of all centrifuge experiments performed as part of this project. A comprehensive set of detailed reports and drawings (Cappa et al. 2014 a,b) along with test data for all experiments listed in Table 1 are available at the NEES project warehouse under project #1161: http://nees.org/warehouse/project/1161. This manuscript will focus on the presentation of the two large scale investigations performed on the 9-m radius centrifuge and describes the model setup and construction, model materials, instrumentation, data acquisition and data processing/storage as well as sample data obtained from both large scale investigations. Hereafter, and in consistency with the NEES data repository, investigation 1 will be labeled RCK01 and investigation 2 is named RCK02 accordingly following the NEES@UCDavis convention of identifying each investigation by the lead investigator's initials. The primary difference between the two investigations is the peat layer thickness and its impact on the seismic response of the levee-peat system.

Table 1. Summary of centrifuge experiments performed as part of this study.

Investigation	Experiment	Centrifuge Radius	Brief Description*	DOI
Small Scale Investigations	1	1m	Peat slurry under surcharge.	10.4231/D32V2C96M
	2	1m	Peat passed through #4 sieve, under surcharge.	10.4231/D3TD9N80K
	3	1m	Peat processed through blender, under surcharge.	10.4231/D3PN8XF79
	4	1m	Peat passed through #4 sieve, no surcharge.	10.4231/D3JW86N3J
	5	1m	Peat passed through #4 sieve, no surcharge.	10.4231/D3F47GT8M
	6	1m	Sandy levee on peat shaken by SGM.	10.4231/D39C6S14W
	7	1m	Sandy levee shaken by SGM.	10.4231/D35M62704
	8	1m	Consolidation of peat under a sand layer.	10.4231/D31V5BD6C
	9	1m	Sandy levee on peat shaken by SGM.	10.4231/D3X63B55H
	10	1m	Sat. sandy levee constructed on arm by water pluviation.	10.4231/D3Z31NP21
	11	1m	Clay levee on peat shaken by SGM sequence.	10.4231/D3G73748K
RCK01	12	9m	Clay levee on peat shaken by SGM sequence.	10.4231/D34M91B6S
	13	9m	Saturated sandy levee on peat shaken by MGM.	10.4231/D30V89J2N
RCK02	14	9m	Clay levee on peat shaken by SGM sequence.	10.4231/D3W37KW7Z
	15	9m	Saturated sandy levee on peat , MGM & aftershocks.	10.4231/D3RB6W337

** SGM = Strong Ground Motion, MGM = Moderate Ground Motion*

EXPERIMENTAL CONFIGURATION FOR RCK01 AND RCK02

The general test setup of the levee systems is depicted in Figure 1. Each configuration consisted of a drainage layer of coarse sand with thickness *D* at the bottom of the model, followed by a peat layer with varying thicknesses (*H*) and a model levee consisting of (a) modeling clay or (b) saturated sand, with geometries as indicated in Figure 1. The levee system was constructed inside a rigid wall container with dimensions of 175.8 cm in length, 90.9 cm in width and 53.7 cm in height (Figure 2a). The rigid container has transparent side walls to enable the acquisition of videos during testing, which was important for this project and outweighed the undesired boundary conditions imposed at the rigid soil/container contact. Figure 2b shows the placement of the container on the centrifuge arm with its respective global coordinate system.

Each of the two large scale investigations (RCK01 and RCK02) consisted of two Experiments: (1) a levee composed of non-liquefiable modeling clay rests on soft peat and several ground motions and sinusoidal sweeps are applied in flight to observe the seismic performance of the peat and the levee-peat interaction (Experiments 12 & 14 in Table 1); (2) the clayey levee is removed and substituted with a saturated sandy levee, and subsequently subjected to the target ground motion to investigate the system behavior (interaction & liquefaction) (Experiments 13 & 15 in Table 1). Model configurations for these four experiments are shown in Figures 3 through 6. The high compressibility of the peat resulted in significant settlement of the levee during spin-up, and Figs. 3 through 6 depict the models in their configurations during testing, with dashed-lines indicating the pre-spin-up model geometry.

The prototype system consists of a 5 m tall levee resting atop top of a 9.5 m and 6 m thick layer of soft peat for RCK01 and RCK02, respectively. The models were spun to a centrifugal acceleration of 57g, therefore the model scale dimensions were a 9 cm tall levee resting atop 16.5 cm and 10.5 cm of peat for RCK01 and RCK02, respectively. The peat thickness during RCK01 was selected to match conditions at a site on Sherman Island where a previous field testing program was conducted on a non-liquefiable model levee using the UCLA eccentric shaker (Reinert et al. 2014). Figure 7 shows photographs of the clayey levee resting atop the peat for RCK01 and RCK02 before the container was installed on the centrifuge arm.

MATERIAL CHARACTERIZATION

The five soil materials utilized in the test setup include peat, modeling clay for the nonliquefiable levees, loose Nevada sand for the liquefiable levees, coarse dense sand beneath the peat, and loam placed atop the liquefiable levee for erosion protection. Additionally, viscous fluid was used to scale the prototype permeability of the liquefiable sandy levee.

Peat

Bulk samples of peat were recovered from depths of 2-3 m at the field test site on Sherman Island in the Sacramento-San Joaquin Delta documented by Reinert et al. (2014). The samples were stored in plastic-lined metal barrels filled with water at UC Davis. Prior to placement in the model container, the material was hand processed to remove coarse particles and long fibers that are unsuitable for use in relatively small centrifuge models. Careful handling was important to avoid the loss of fluid in the fibers due to squeezing and to obtain a homogeneous and soft soil matrix. The peat was maintained submerged during model construction. Important material characteristics of the processed peat were determined via laboratory studies (Cappa et al., 2015). Additional in-situ test results of the peat from geophysical testing, hand augering and cone penetration testing (CPT) are available in Reinert et al. (2014).

The peat had a specific gravity G_s of 1.79 and an average organic content, OC, of 64%. Across an overburden pressure range of 5-150 kPa, the virgin compression index C_c and the recompression index C_r were determined to be 3.9 and 0.4, respectively. Two sets of bender elements recorded shear wave velocities at accelerations of 1, 5, 10, 20, 40, and 57g during spin-up, thereby enabling characterization of the shear wave velocity as a function of confining pressure. Figure 8 presents a sample measurement of shear wave velocities during RCK02 at 57g. The bender elements exhibited capacitive coupling with the conductive peat soil, and the desired elastic wave signal is superposed on an undesired portion of the signal corresponding to capacitive decay. The travel time corresponding to first arrival of the shear wave can nevertheless be measured from the two receivers, enabling calculation of the shear wave velocity. Equation 1 is a general form for characterizing shear wave velocity as a function of vertical effective stress, σ_v'.

$$V_s = V_{s1} \cdot \left(\frac{\sigma_v'}{p_A} \right)^n \qquad (1)$$

By plotting shear wave velocities measured across a range of centrifugal accelerations, the parameters V_{s1} and n can be determined via least squares regression, as shown in Figure 9. In the peat, V_{s1} and n were found to be 33 m/s and 0.31, respectively.

P-wave velocity was measured by gently striking the top of the modeling clay levee and measuring the downward-propagating compressive wave using vertical accelerometers. The p-wave velocity of the peat was found to be approximately 419 m/s in RCK01 and approximately 172 m/s in RCK02. Both measurements indicate that the peat was unsaturated. This is consistent with field conditions, in which the peat holds a significant amount of entrapped gasses due to its past and ongoing decomposition.

A miniature CPT test was performed in-flight during RCK02, measuring tip resistance over a depth range of 27 cm (Figure 10). The CPT apparatus was placed in the free field region during Experiment 14 and was pushed through the mid-point of the upstream levee slope during Experiment 15. The free-field peat exhibited a very low tip resistance that increased slightly with depth, reaching a maximum near 0.24 MPa at the bottom of the peat layer. The relatively low tip resistance is due to low consolidation stresses in the free field. By contrast, the resistance in the peat beneath the sandy levee was significantly higher, increasing from about 0.5 MPa at the top of the peat to 1.0 MPa at the bottom of the peat. Consolidation stresses from the overlying levee clearly increased the peat strength. Tip resistance increased dramatically below the peat as the CPT probe pushed into the dense coarse sand.

Liquefiable Sandy Levee (Nevada Sand)

The liquefiable levee fill (Experiments 13 and 15, Table 1) consisted of saturated Nevada sand with a mean grain size D_{50} of 0.14 mm, a specific gravity G_s of 2.66, a maximum and minimum void ratio $e_{max/min}$ of 0.78 and 0.51 respectively, a coefficient of uniformity C_u of 2, and a hydraulic conductivity k of approximately 10^{-3} cm/s in non-viscous water (Dashti 2009). The fines content passing # 200 sieve was removed from the sand. Shear wave velocity measurements of the material obtained during the second investigation (RCK02) suggested shear wave velocity parameters V_{s1} and n of 151 m/s and 0.23, respectively. To obtain well saturated sand capable of simulating undrained shearing behavior during liquefaction, traditional vacuum saturation techniques normally used in centrifuge modeling were not suitable for our application because the gasses in the peat would expand under vacuum, thereby resulting in model disturbance. A device was therefore developed to pre-saturate the sand and the saturated sand was subsequently water pluviated into the model without air contact. The device consists of an acrylic vacuum chamber with a hose attached at the bottom, and details can be found in Yniesta et al. (2015). The relative density, D_R, of the sand placed by this method was 27 – 58%, with an average density of 42% and a standard deviation of 8.3%. This density range matches well with D_R values of 30 -50% observed in non-engineered hydraulic fill in the field. Water pluviation has the benefit of matching the manner in which many liquefiable sand deposits are placed. Fabric is known to exert a significant influence on liquefaction potential of sand (Abdun et al., 2013).

Coarse Dense Sand (Monterey Sand)

A coarse sand layer consisting of #0/30 Monterey Sand was placed at the bottom of the container to represent the natural geologic strata typical for the Delta, and to provide drainage at the bottom of the peat layer during consolidation. The granular material was dry pluviated to a relative density of 90%, thereby preventing liquefaction during shaking. A chimney drain constructed of the same coarse sand material was placed along the south wall of the container (Figure 1). Dashti (2009) determined this particular material to have a grain size D_{50} = 0.40 mm, a coefficient of uniformity C_u = 1.3, a specific gravity G_s of 2.64, and a maximum/minimum void ratio $e_{max/min}$ of 0.843 and 0.510, respectively. The hydraulic conductivity (k) is approximately 10^{-2} cm/s. Shear wave velocity parameters $V_{s,1}$ and n were 195 m/s and 0.26, respectively.

Modeling Clay

Impermeable, oil based modeling clay with a unit weight γ of 18 kN/m^3 was formed into a clayey levee by pouring molten clay into a mold. The clay levee was moderately deformable, allowing for small differential settlements in flight. Shear wave velocity of the modelling clay measured at 1g was about 400 m/s, and this is anticipated to be the same as the shear wave velocity in-flight since the modelling clay does not consolidate during spin-up.

Loam Layer atop the Sandy Levee Fill

To provide erosion protection, and to better visualize the crack and deformation patterns of the sandy levee during testing, the liquefiable levee fill was covered with a dry-pluviated, 1.5cm thick mixture of 75% Yolo loam and 25% Monterey sand (by mass). This particular loam is frequently found in the Sacramento region and was excavated from an open area at the centrifuge facility.

Viscous Pore Fluid

The liquefiable sandy levees were saturated with a viscous pore fluid to provide undrained loading conditions during shaking. The viscosity of the methylcellulose/water mixtures was 14 cSt and 18 cSt (1 centistokes = 1 mm^2/s) for RCK01 and RCK02, respectively. Measurements were taken at 20°C prior to testing. Water expelled during consolidation of the peat mixed with the viscous fluid, resulting in a post-test viscosity of about 4 cSt in the free fluid in the channel. However, we believe that the fluid inside the levee fill was not prone to this mixing, and therefore the viscosity remained high.

MODEL CONSTRUCTION AND LOAD APPLICATION

The coarse dense sand stratum at the bottom of the model was dry pluviated in two lifts to accommodate placement of sensors after the first lift. The sand was water saturated by pouring water on a sponge resting on the sand surface.

Peat slurry was then poured from buckets onto the sand and smoothed with trowels at elevations where sensors would be placed. The amount of peat slurry required to achieve the target peat thickness after consolidation in-flight was based on observations from the

Shaevitz centrifuge test program (Cappa et al. 2015), laboratory consolidation studies (Shafiee et al. 2013), and settlement predictions using Settle 3D (Rocscience 2014). The peat slurry was too weak to support the clay levee, so a layer of Nevada sand (γ_{dry} = 17 kN/m^3) was placed on top of the peat to pre-consolidate the material over the course of three days. The thickness of the Nevada sand was 3.5 cm for RCK01 and 9 cm for RCK02. Following the pre-consolidation at 1g, the Nevada sand layer along with the expelled water was removed and the clayey levee was placed on a thin geotextile atop the peat. Based on anticipated settlement of the peat beneath the levee, peat was removed from the free-field to achieve an approximately horizontal peat surface after consolidation at 57g (Cappa et al. 2014 a&b). Final construction steps included the installation of lights, attachment of racks for sensor instrumentation, placement of all external sensors and CPT, installation of video cameras and connection of all instrumentation to the data acquisition system.

Centrifuge spin-up proceeded incrementally to avoid undrained bearing failure of the peat. Pore pressures in the peat beneath the levee were monitored to guide the spin-up rate. This procedure is similar to staged construction techniques commonly utilized to construct embankments on soft foundations (e.g., Ladd 1991), except that the gravity load is staged rather than the fill height. The clayey levee was tested for two consecutive days in RCK01 (as described in Table 2), dedicated to consolidating the peat for several hours at various g-levels (day 1) and applying a series of ground motions with different peak base accelerations at 57-g (day 2). During investigation RCK02 the clayey levee test required only one day because the peat thickness was less and consolidation therefore required less time.

During spin-up, the levees settled significantly and became submerged in water expelled from the peat. We originally intended to pump the expelled water out of the models to bring the water table near the surface of the peat. However, the pumping system failed during RCK01, and we elected to test RCK02 with the free water in place to facilitate comparison with RCK01. Furthermore, during spin-down the peat swelled back to near its initial position, re-absorbing the expelled water. If this water were pumped out, the peat could have become desiccated during spin-down and we wished to maintain saturation of the peat for the sandy levee experiments.

Upon test completion, the clayey levee was removed and replaced with a sandy levee. A 10 cm wide drainage blanket consisting of coarse sand wrapped with filter paper was placed beneath the downstream toe of the levee to prevent piping erosion and maintain the phreatic surface within the levee prism. The container was filled with viscous fluid and the sandy levee was pluviated into the model. Vertical sheet metal barriers constrained the pluviated sand within the desired footprint area, and the levee was then manually re-shaped to the desired geometry. The sandy levee was constructed with a 3:1 slope on the dry side to reduce the amount of erosion due to seepage during flight and to represent typical levee conditions in the field. The upstream slope was constructed with a 2:1 angle. After water pluviation, the fluid was slowly siphoned from the dry-side of the levee.

During spinning, viscous water that seeped through the levee was collected in a U-shaped ditch installed in the downstream peat, and collected fluid was pumped back to the channel to maintain a steady-state seepage condition. Furthermore, a spillway was installed in the levee to regulate the elevation of the channel relative to the levee crest and prevent over-topping during spin up as the levee settled. For RCK01, the spillway was formed of a stiff metal U-channel that settled less than the levee during consolidation, resulting in erosion of the sand from beneath the channel. As a result, the water table was hydrostatic. A more flexible spillway was implemented in RCK02, enabling a channel to be maintained on one side of the levee.

Loading

Table 2 summarizes the base excitations applied to the models for both investigations. The organization of data into trials and repetition follows NEES requirements. Applied ground motions include: (1) scaled versions of ground motions recorded during the 1989 Loma Prieta Earthquake at the USCS/Lick Lab, Ch. 1 – 90°, and the 1995 Kobe Earthquake recorded at a depth of 83 m at the Port Island downhole array, (2) low-amplitude step waves imposed primarily to verify sensor function, and (3) sine sweeps intended to characterize the dynamic response of the model. The magnitudes of the Loma Prieta and Kobe earthquakes are in the range that contributes the most to seismic hazard in the Delta (DRMS 2009). Scaled versions of these motions with amplitudes ranging from 0.006g to 0.52g in prototype scale were imposed on the base of the model container.

Table 2. Base Excitation Summary.

Investigation	Experiment	Trial	Repetition	Date	Time Stamp	Description	Peak base acceleration, PBA (g) in prototype scale
RCK01	12	1	1	11/4/2013	12:01:51	Slow data file for first spin	-
	12	1	2	11/4/2013	15:36:41	Slow data file for first spin	-
	12	1	3	11/4/2013	9:26:00	Rpm record	-
	12	2	1	11/4/2013	15:50:46	Step wave 1	0.006
	12	3	1	11/5/2013	10:18:50	Slow data file for second spin	-
	12	4	1	11/5/2013	13:25:45	Step wave 2	0.006
	12	5	1	11/5/2013	14:03:14	Sine sweep 1	0.021
	12	6	1	11/5/2013	14:31:51	Small Loma Prieta	0.036
	12	7	1	11/5/2013	14:45:16	Small Kobe	0.034
	12	8	1	11/5/2013	14:57:21	Medium Loma Prieta	0.174
	12	9	1	11/5/2013	15:13:14	Medium Kobe	0.194
	12	10	1	11/5/2013	15:39:51	Large Kobe	0.491
	12	11	1	11/5/2013	16:29:07	Large Loma Prieta	0.476
	12	12	1	11/5/2013	17:13:39	Sine sweep 2	0.021
	13	1	1	11/21/2013	10:31:08	Slow data file for second spin	-
	13	2	1	11/21/2013	14:43:30	Step wave 3	0.005
	13	3	1	11/21/2013	14:50:49	Moderate Kobe	0.375
RCK02	14	1	1	2/27/2014	7:53:12	Slow data file for first spin	-
	14	2	1	2/27/2014	12:50:38	Step wave 1	0.006
	14	3	1	2/27/2014	13:01:20	Sine sweep 1	0.018
	14	4	1	2/27/2014	13:45:13	Large Kobe	0.526
	14	5	1	2/27/2014	16:27:04	Large Loma Prieta	0.439
	14	6	1	2/27/2014	17:23:09	Sine sweep 2	0.020
	14	7	1	2/27/2014	17:37:01	Step wave 2	0.007
	14	8	1	2/27/2014	17:45:34	Medium Kobe	0.270
	14	9	1	2/27/2014	17:54:24	Small Kobe	0.131
	15	1	1	3/12/2014	12:00:21	Slow data file for second spin	-
	15	2	1	3/12/2014	17:04:41	Step wave 3	0.006
	15	3	1	3/12/2014	17:17:15	Moderate Kobe	0.336
	15	4	1	3/12/2014	17:33:41	Small Kobe	0.101
	15	5	1	3/12/2014	17:43:42	Very small Kobe	0.057

INSTRUMENTATION

Sensors used to characterize model response include accelerometers [PCB Piezotronics, models 352B68, 352C68, 352M54, 355M69, 353B18 & 353B31; range: 50g, 100g and

500g], pore pressure transducers [Keller, model 2Mi-100-81840 range: 0 - 689.5kPa], linear potentiometers (L) [BEI Duncan, models: 606R6KL.12 & 604R4KL.15, stroke: 10cm and 15cm], and bender elements [Piezo Systems Inc., 2 layer transducer with PSI-5A4E piezoceramic (nickel electrodes) and brass center reinforcement]. The general instrumentation layout for each experiment is shown in Figures 3-6. Accelerometers and bender elements were coated with a waterproofing layer prior to being placed into the model. Linear potentiometers were attached to a rack mounted to the top of the container. Vertical linear potentiometer rods rested on small footing plates to prevent penetration into the soft soil. Horizontal linear potentiometer rods were attached to a metal frame cantilevered from the soil. These horizontal linear potentiometers provide accurate low frequency response for measuring permanent ground deformations, but the metal frame alters the high frequency response. The high frequency response is typically obtained from an accelerometer embedded in the soil near the anchor frame. Some of the accelerometers were fastened to a right-angle connector to maintain a 90° angle between sensors, which sometimes tend to shift during model construction and/or testing on the centrifuge. The position of each sensor was measured during installation and again during excavation following testing. Tables containing sensor positions, orientations, serial numbers, calibrations and measurements are available at the NEES project warehouse. Some of the sensors ceased to function properly during experimental activities, and a list of such sensors is available in the NEEShub repository. Loss of sensor functionality is a natural part of experimental testing, and only a small fraction of the sensors failed to function properly.

A total of eight cameras supported the surveillance of the specimen behavior during flight. Two high speed cameras captured the behavior of the levee from the east and west side of the container during the application of the ground motions. The models were also documented by photographs taken during construction and testing, and a time-lapse video of the model construction sequence was constructed from automated photos recorded at set time intervals. All videos, photos, and construction time lapses are available on the NEEShub repository.

DATA PROCESSING AND ARCHIVING

Experimental data are categorized as "Unprocessed Data", "Converted Data", and "Corrected Data" in accordance with NEES standards. Experimental data is further categorized as "slow data" sampled at 1 Hz during spin-up, spin-down and between ground motion applications, and "fast data" sampled at 4167 Hz during the application of ground motions. Slow data helped observe the low frequency response of the model and time dependent consolidation settlement of the peat, while fast data captured the dynamic response of the model during base excitation. For each experiment, Trial 1 contains the slow data while Trials 2 and higher contain fast data.

Unprocessed Data

Unprocessed data are in engineering units in binary format. Prior to testing, a calibration file is uploaded to the data acquisition system, and the recorded voltage signals are then automatically converted to engineering units. All recordings are in model scale. A LabView virtual instrument (vi) file is required to view the binary data files, and we do not anticipate users will download and utilize this data. It is archived for completeness, and compliance with NEES standards.

Converted Data

The Unprocessed Data are then converted from binary to ASCII format and saved as text files in the "Converted Data" folder in the NEES repository. Generally, zero voltage does not correspond to a value of zero for the engineering quantity being measured. For example, the rod of the vertical linear potentiometers measuring settlement of the levee were initially retracted as far into the housing as possible to facilitate the maximum possible useful range for these sensors during consolidation. A fully retracted linear potentiometer returns a non-zero voltage. Therefore the reference condition corresponding to zero settlement does not correspond to zero voltage. In accordance with NEES standards, offsets are not applied to Converted Data. For this reason, we anticipate that users will not utilize the Converted Data as the primary data source, and it is archived for completeness and compliance with NEES standards.

Corrected Data

Corrected Data are the data files that we anticipate will be most useful to users of the curated dataset. The following operations are applied to the Converted Data to obtain Corrected Data:

(i) Offsets were applied such that zero corresponds to a desired reference condition. Specifically, the mean value was subtracted from all acceleration records, and the initial value prior to spin-up was subtracted from all displacement and load cell records. Offsets to pore pressure transducers were set such that zero corresponds to atmospheric pressure. During testing, some of the linear potentiometer rods fell off the bearing pads, resulting in an abrupt offset in the settlement record. These offsets were removed from the corrected linear potentiometer data.

(ii) The data were sorted such that they are grouped by sensor type in ascending numerical order (e.g., A1, A2, A3, …, L1, L2, L3, …). The unprocessed and converted data files are ordered in accordance with the data acquisition channel used to collect the data, but this order is inconvenient for interpreting the data.

(iii) The data files were truncated to remove excess data collected before and after shaking to reduce file size. Typically, 15 seconds of data are collected for each fast data file, but only approximately 1 second corresponds to the shaking event. Enough pre- and post-event data are left in the signals to facilitate proper interpretation of the dynamic processes. However, the data files are too short to monitor pore pressure dissipation following long shaking events, and the slow data should be used for this purpose.

(iv) Sign conventions were assigned to the data quantities to maintain consistency with the global coordinate system. Furthermore, centrifuge scaling factors are applied to the data to produce prototype units. The centrifugal acceleration was 57g for all experiments, and appropriate scale factors followed Kutter (1992).

SAMPLE DATA

This section presents sample data to illustrate interesting features of the test and demonstrate data quality. More complete presentation of the experimental data to support conclusions from the experimental study is reserved for future publications.

Figure 11 shows slow data quantities including centrifuge g-level, pore pressure, and settlement for Experiment 15 for a duration of time that encompasses spin-up, application of a step wave and three ground motions, and spin-down. The model was spun up in increments until the target acceleration of 57-g was reached, with each increment approximately doubling the g-level. The incremental spin-up permitted pore pressures in the peat to decrease, and undrained shear strength to increase, so that the peat could support the load imposed by the levee. This process took approximately 3 hours. After reaching the target g-level, the model was permitted to consolidate for about one hour. As pore pressures decreased, settlement continued to increase due to primary consolidation and secondary compression in the peat, and the levee showed signs of distress as a result of this settlement. The ground motions were imposed before the levee accumulated too much distress, and P6 was still decreasing slightly at this time. The total consolidation settlement measured at the levee crest prior to the application of the first ground motion was 55 mm (LP 14), while 35 mm of settlement occurred in the free-field.

The moderate Kobe motion had a peak base acceleration of 0.38g, and the levee fill liquefied and slumped, resulting in a breach with water from the channel pouring over the levee and eroding it away until the water elevation equalized on both sides of the levee (Figure 12). Settlements at the levee crest measured 13 mm to 16 mm in model scale, which translates to 0.71 m – 0.91 m in prototype. Videos capturing the liquefaction process and sandy levee failure are available on the NEES project warehouse.

The excess pore pressure within the levee fill recorded by P9 abruptly rises during application of the Kobe motion and quickly dissipates due to the high permeability of the sand, whereas the excess pore pressure in the peat beneath the levee decreases slowly after the ground motion. Pore pressure in the free-field on the landward-side of the levee abruptly increases and remains elevated. This is due to the water in the channel being released, thereby permanently elevating the groundwater table on the landward free-field side of the levee.

Two more ground motions with smaller amplitude were applied after the moderate Kobe motion to observe the threshold for liquefaction triggering in the levee fill and to simulate aftershocks. These motions induced a measurable pore pressure and settlement response.

Fast data recorded during the moderate Kobe motion are shown in Figure 13, including acceleration, pore pressure, and settlement, all in prototype units. The peak base acceleration was 0.38g and the peak acceleration of the levee crest was 0.28g, indicating that the soil profile de-amplified the input motion. The pore pressure in the center of the sandy levee increased by approximately 30 kPa, which is equal to the initial vertical effective stress at the levee center, indicating the levee fill liquefied. Pore pressures in the sand remained elevated for the duration of shaking, then dissipated quickly after shaking ceased. Excess pore pressure in the peat beneath the levee exhibited a dynamic response during shaking and a net reduction from the beginning to the end of shaking. This pore pressure response is caused by a combination of shearing and changes in total stress as the levee breached and water flowed over the top. Settlement records exhibit significant high frequency noise, but a dynamic response is evident superposed on the noise, and the permanent component is clear. The levee crest settled 0.7 m at the position of LP 14, which is near the center of the levee. The breach occurred where settlement was highest, between the center of the levee and the container wall.

SUMMARY AND CONCLUSIONS

This data paper describes the research objectives, test setup, instrumentation and data organization of a series of centrifuge tests performed at the NEES@UC Davis equipment site performed between January 2013 - March 2014. Eleven small scale centrifuge experiments and four large scale centrifuge experiments studied the seismic behavior of levee-peat systems. Test data are achieved in the NEES project warehouse are assigned digital object identifiers, and we recommend using the corrected data.

Potential uses of the data presented herein includes:

(i) Study the post-cyclic volume change potential of peat, which is a previously unidentified mechanism that has been recently studied in the laboratory (Shafiee et al. 2015). Laboratory results indicate the potential for a secondary compression clock reset due to cyclic shearing of the peat with shear strains higher than 1%. This would contribute to an increase in the rate of settlement of the levee fill following strong shaking. Centrifuge test data will provide useful benchmarks to validate the laboratory outcomes given the wide range of shear strain levels achieved during cyclic loading.

(ii) Evaluate the dynamic response of the clayey levee using concepts derived from soil-structure interaction. The clay levee is stiff in comparison with the underlying peat, thereby mimicking a stiff structure resting atop soil. The levee was observed to translate and rock on top of a softer underlying layer, thereby altering the stress and strain distribution in the levee fill and in the underlying peat. Vibration modes were presented by Cappa et al 2015 using transfer functions for translation and rocking.

(iii) Study the influence of the peat and levee geometry on liquefaction potential of the levee fill. Traditional liquefaction triggering procedures assume one-dimensional wave propagation by assuming that the cyclic stress ratio is related to peak horizontal acceleration. However, the peat permits the levee to rock, thereby resulting in principal stress directions that differ from one-dimensional wave propagation. The influence of these stress rotations is currently not well understood.

(iv) Validation of numerical simulations. The development of a nonlinear constitutive model for peat is currently underway. The model focuses on matching the creep behavior of peat, and its damping behavior. This includes the increase of secondary compression rate due to cyclic loading. The model extends the one-dimensional hardening law described in Yniesta et al. (2015), to three-dimensional loading conditions.

ACKNOWLEDGEMENTS

This research was funded by the National Science Foundation under grant # NSF-NEESR CMMI 1208170. This material is based upon research performed in a renovated collaboratory by the National Science Foundation under Grant No. 0963183, which is an award funded under the American Recovery and Reinvestment Act of 2009 (ARRA). The writers would like to acknowledge the valuable assistance and technical support of the UC Davis Centrifuge facility team along with the undergrad and graduate students that assisted in laboratory and model testing

REFERENCES

Abdoun, T., Gonzalez, M., Thevanayagam, S., Dobry, R., Elgamal, A., Zeghal, M., Mercado, V., and El Shamy, U. (2013). ”Centrifuge and Large-Scale Modeling of Seismic Pore Pressures in Sands: Cyclic Strain Interpretation.” *J. Geotech. Geoenviron. Eng.*, 139(8), 1215–1234.

Cappa, R., Yniesta, S., Brandenberg, S., Stewart, J. and Lemnitzer, A., (2014a) “NEESR: Levees and Earthquakes: Averting and Impending Disaster- Data Report for Centrifuge Experiments 12L and 13L”. Final Project Report (https://nees.org/warehouse/project/1161)

Cappa, R., Yniesta, S., Brandenberg, S., Stewart, J. and Lemnitzer, A., (2014b) “NEESR: Levees and Earthquakes: Averting and Impending Disaster- Data Report for Centrifuge Experiments 14L and 15L”. Final Project Report (https://nees.org/warehouse/project/1161)

Cappa, R., Yniesta, S., Lemnitzer, A., Brandenberg, S., and Shafiee, A. (2015) Settlement Estimations of Peat during Centrifuge Experiments. *Proceedings, IFCEE 2015*: pp. 152-160. doi: 10.1061/9780784479087.016

Dashti, S. (2009). "Toward Developing an Engineering Procedure for Evaluating Building Performance on Softened Ground", *Ph.D. Thesis, University of California, Berkeley, CA.*

DRMS, URS Corporation and Jack Benjamin and Associates Inc. (2009). "*Delta Risk Management Strategy. Phase 1 Final Report.*" California Department of Water Resources.

Experiment-12: Riccardo Cappa, Samuel Yniesta, Scott Brandenberg, Jonathan Stewart, Anne Lemnitzer (2014). TEST 12L - RCK01 : Part 1 - 9m radius centrifuge experiment on clayey levee behavior underground motions. Network for Earthquake Engineering Simulation (NEES)(distributor). Dataset. *DOI: 10.4231/D34M91B6S*

Experiment-13: Riccardo Cappa, Samuel Yniesta, Scott Brandenberg, Jonathan Stewart, Anne Lemnitzer (2014). TEST 13L - RCK01 : Part 2 - 9m radius centrifuge experiment on sandy levee behavior underground motion. Network for Earthquake Engineering Simulation (NEES)(distributor). *Dataset. DOI: 10.4231/D30V89J2N*

Experiment-14: Riccardo Cappa, Samuel Yniesta, Scott Brandenberg, Jonathan Stewart, Anne Lemnitzer (2014). TEST 14M - RCK02 : Part 1 - 9m radius centrifuge experiment on clayey levee behavior underground motions. Network for Earthquake Engineering Simulation (NEES)(distributor). *Dataset. DOI: 10.4231/D3W37KW7Z*

Experiment-15: Riccardo Cappa, Samuel Yniesta, Scott Brandenberg, Jonathan Stewart, Anne Lemnitzer (2014). TEST 15M - RCK02 : Part 2 - 9m radius centrifuge experiment on sandy levee behavior underground motions. Network for Earthquake Engineering Simulation (NEES)(distributor). Dataset. *DOI: 10.4231/D3RB6W337*

Kutter, B.L.1992. *Dynamic Centrifuge Modeling of Geotechnical Structures*. Transportation Research Record, TRB, National Research Council, 1336: 24-30.

Ladd, C. C., 1991. "Stability evaluation during staged construction." *J.Geotech. Engrg.*, 117(4), 540–615.

Yniesta, Samuel, Lemnitzer, Anne, Cappa, Riccardo, and Brandenberg, Scott J., 2015. "Vacuum Pluviation Device for Achieving Saturated Sand," *Geotechnical Testing Journal*, Vol. 38, No. 3, 2015, pp. 1–6, doi:10.1520/GTJ20140173. ISSN 0149-6115

Reinert, E., Stewart, J.P., Moss, R.,E.,S., and Brandenberg, S., 2014. "Dynamic Response of a Model Levee on Sherman Island Peat: A Curated Data Set", *Earthquake Spectra*, May 2014, Vol. 30, No. 2 (May 2014) pp. 639-656

Rocscience (2014). Settle 3D – Settlement and Consolidation Analysis. https://www.rocscience.com/products/7/Settle3D

Sasaki, Y. (1994). "Embankment Failure Caused by the Kushiro-oki Earthquake of January 15, 1993", *Special Volume "Performance of Ground and Soil Structures During Earthquakes", 13th International Conference on Soil Mechanics and Earthquake Engineering*, New Delhi, pp.61-68.

Shafiee, A., Brandenberg, S.J. and Stewart J.P. (2013). "Laboratory investigation of the pre- and post-cyclic volume change properties of Sherman Island peat." *Geocongress 2013 -- Stability and Performance of Slopes and Embankments III, San Diego, CA, ASCE Geotechnical Special Publication No. 231, CL Meehan, DE Pradel, MA Pando, and JF Labuz (eds.), Paper No. 560 (electronic file).*

Shafiee, A., Stewart, J.P., and Brandenberg, S.J. (2015). *"Reset of secondary compression clock for peat by cyclic straining."Journal of Geotechnical and Geoenvironmental Engineering*, Vol. 141, No. 3.

LIST OF FIGURES

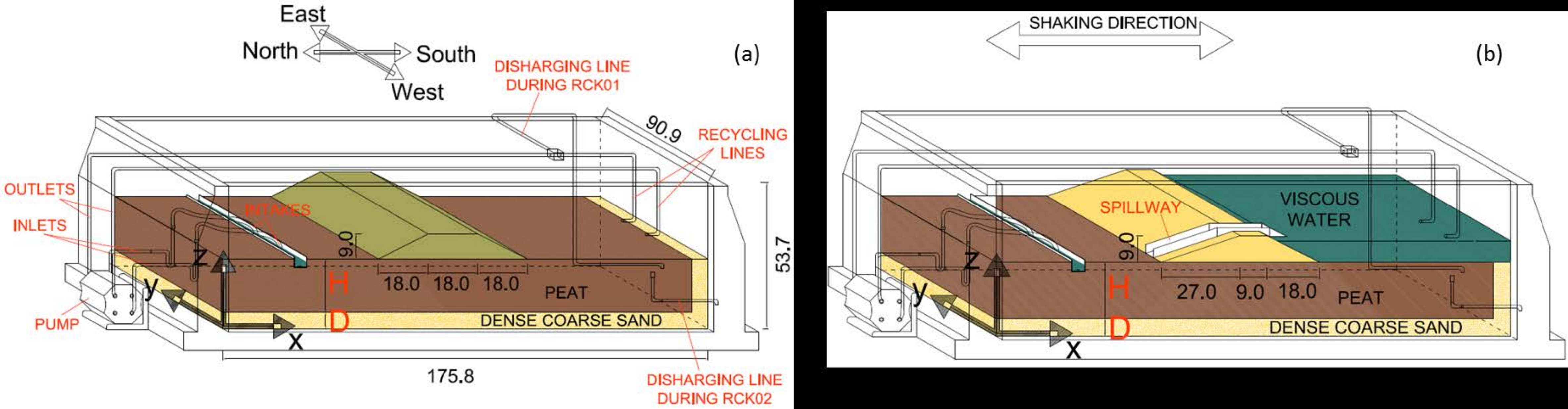
East
North
South
West
(a)
DISHARGING LINE
DURING RCK01
90.9
RECYCLING
LINES
OUTLETS
INLETS
INTAKES
9.0
53.7
18.0
18.0
18.0
H
PEAT
D
DENSE COARSE SAND
PUMP
z
y
x
175.8
DISHARGING LINE
DURING RCK02
SHAKING DIRECTION
(b)
VISCOUS
WATER
SPILLWAY
9.0
27.0
9.0
18.0
H
PEAT
D
DENSE COARSE SAND
z
y
x

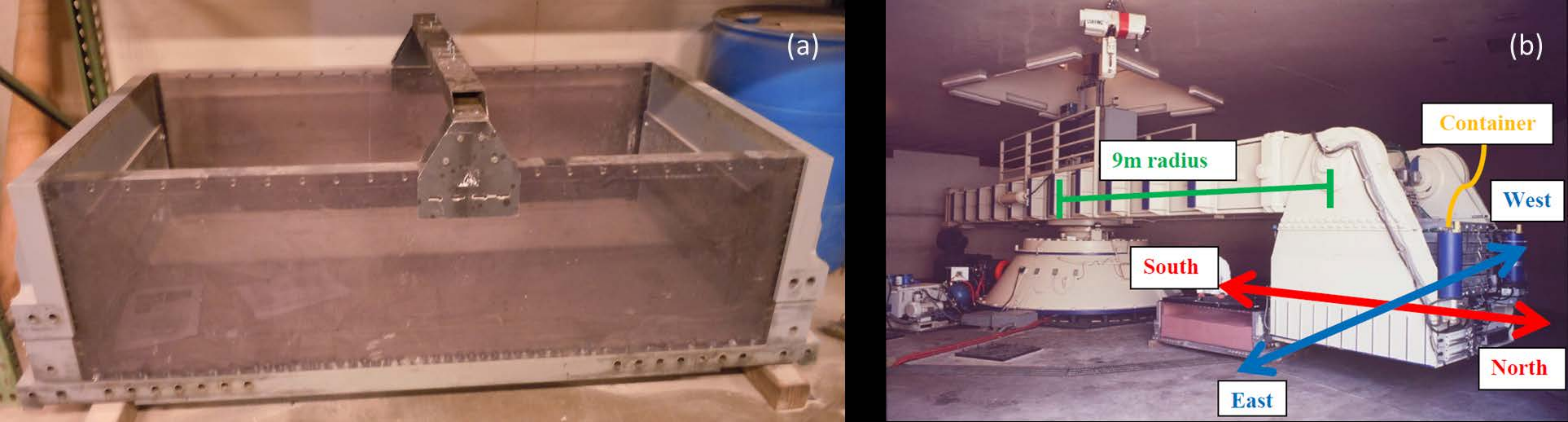
(a)
(b)
Container
9m radius
West
South
North
East

PRODUCED BY AN AUTODESK EDUCATIONAL PRODUCT

PRODUCED BY AN AUTODESK EDUCATIONAL PRODUCT

PRODUCED BY AN AUTODESK EDUCATIONAL PRODUCT

PRODUCED BY AN AUTODESK EDUCATIONAL PRODUCT

PRODUCED BY AN AUTODESK EDUCATIONAL PRODUCT

PRODUCED BY AN AUTODESK EDUCATIONAL PRODUCT

PRODUCED BY AN AUTODESK EDUCATIONAL PRODUCT

PRODUCED BY AN AUTODESK EDUCATIONAL PRODUCT

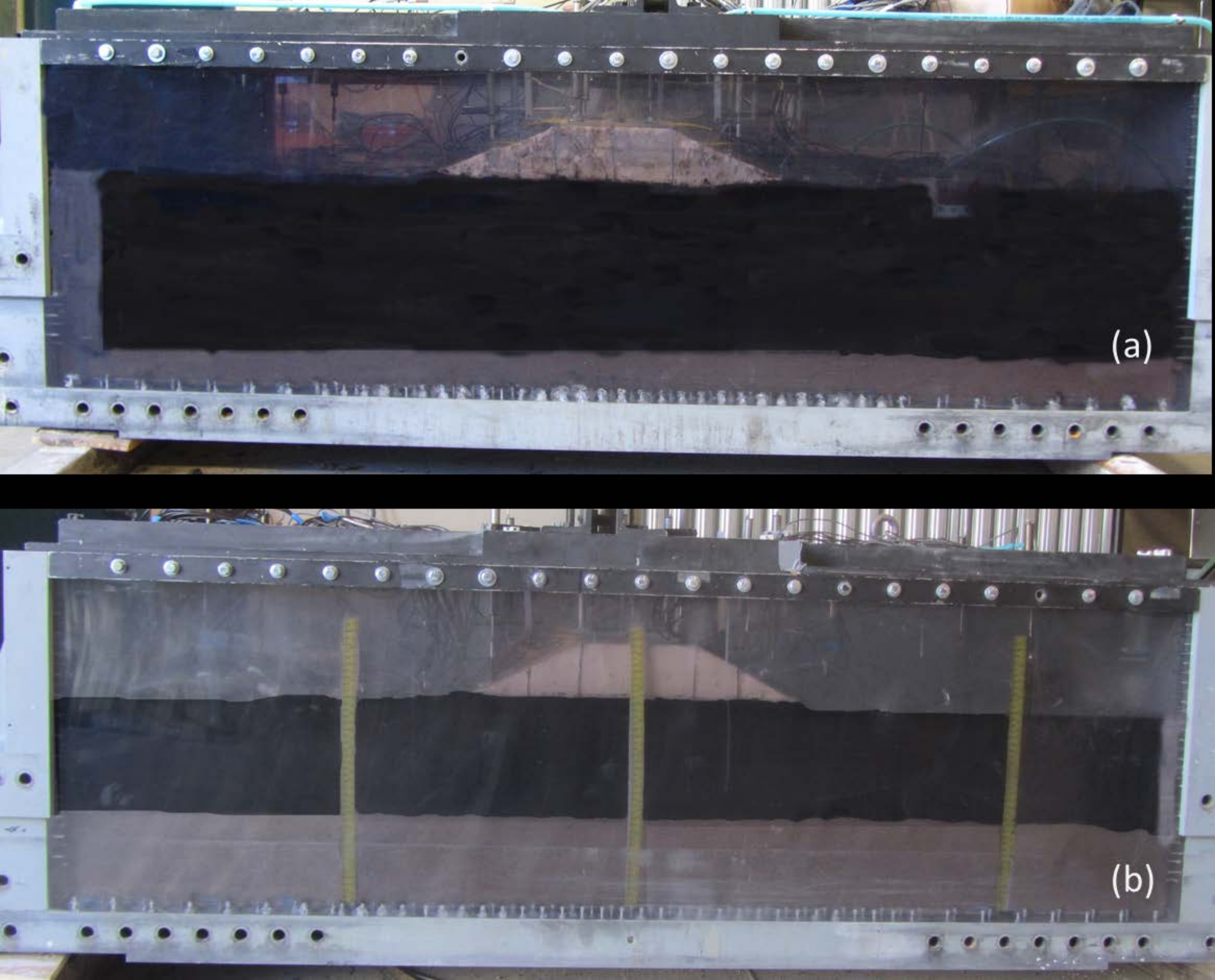
(a)
(b)

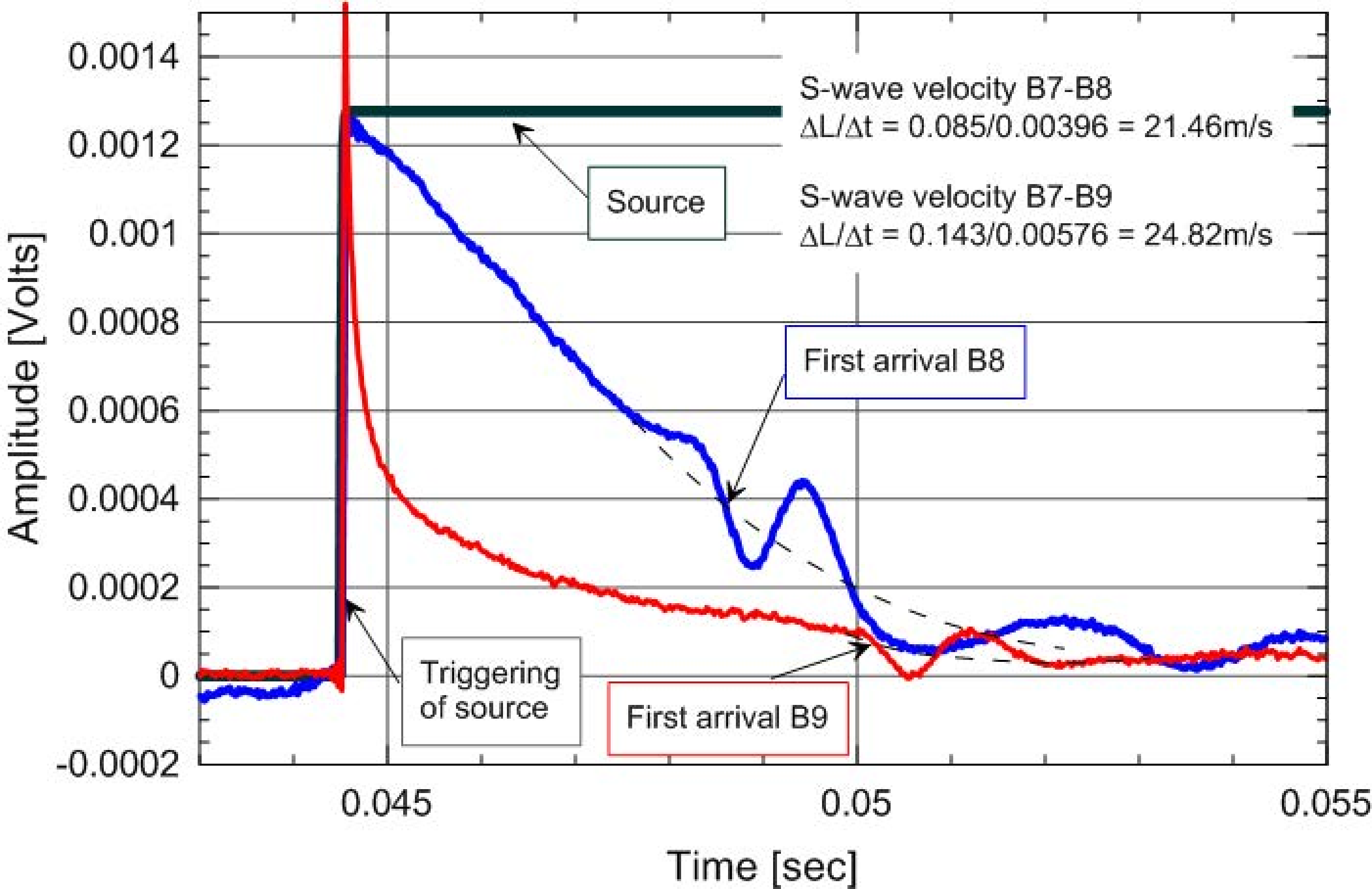

0.0014
0.0012
0.001
0.0008
0.0006
0.0004
0.0002
0
-0.0002
Amplitude [Volts]
0.045
0.05
0.055
Time [sec]
S-wave velocity B7-B8
ΔL/Δt = 0.085/0.00396 = 21.46m/s
S-wave velocity B7-B9
ΔL/Δt = 0.143/0.00576 = 24.82m/s
Source
First arrival B8
Triggering of source
First arrival B9

Fit Results

FIT FOR PEAT
Equation ln(Y) = 0.3055639671 * ln(X) + 3.505815996
Alternate Y = pow(X,0.3055639671) * 33.30861245
Number of data points used = 20
Average ln(X) = -2.35205
Average ln(Y) = 2.78711
Residual sum of squares = 0.399583
Regression sum of squares = 4.86958
Coef of determination, R-squared = 0.924166
Residual mean square, sigma-hat-sq'd = 0.022199

Fit Results

FIT FOR PEAT
Equation ln(Y) = 0.3055639671 * ln(X) + 3.505815996
Alternate Y = pow(X,0.3055639671) * 33.30861245
Number of data points used = 20
Average ln(X) = -2.35205
Average ln(Y) = 2.78711
Residual sum of squares = 0.399583
Regression sum of squares = 4.86958
Coef of determination, R-squared = 0.924166
Residual mean square, sigma-hat-sq'd = 0.022199

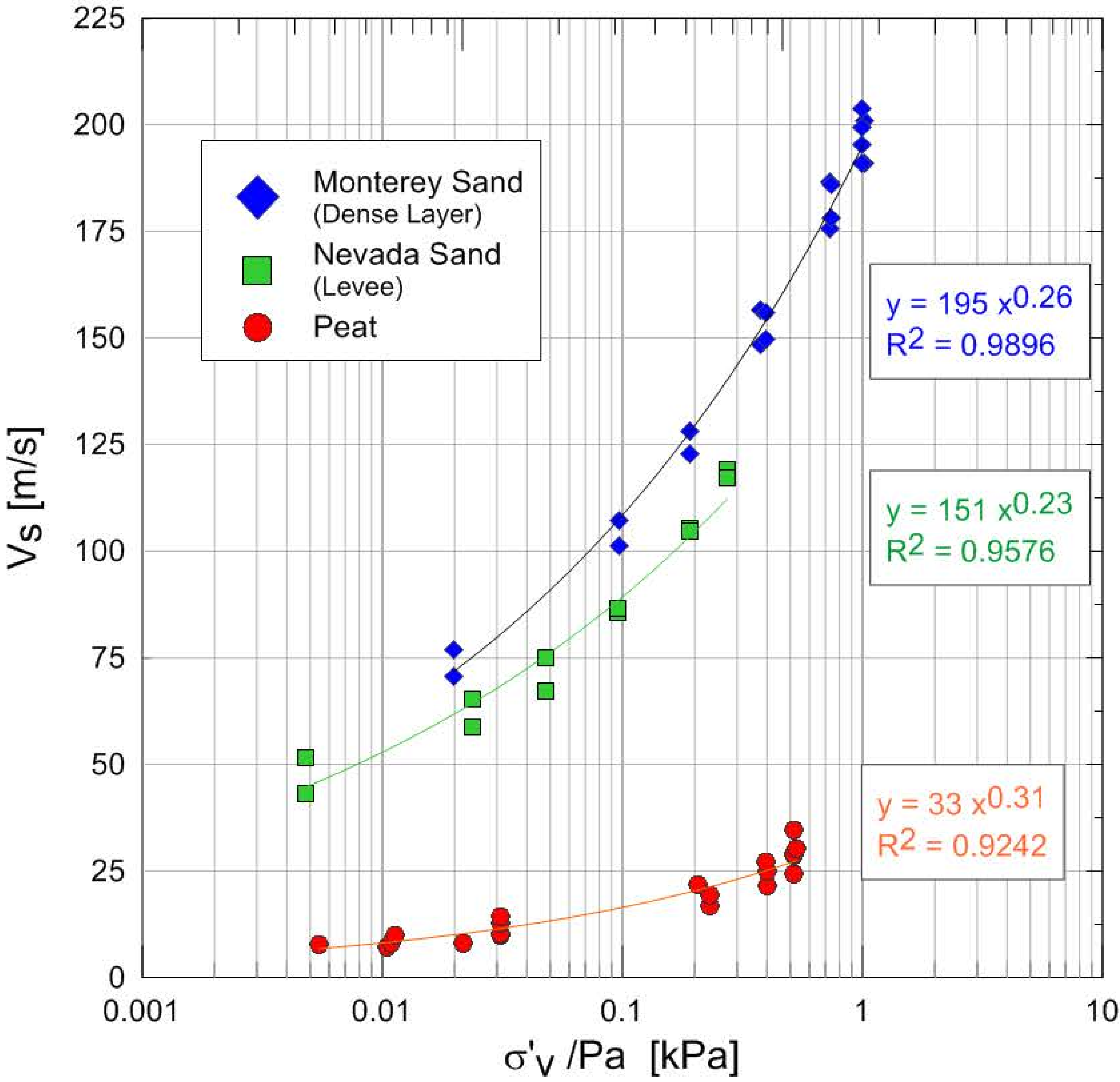

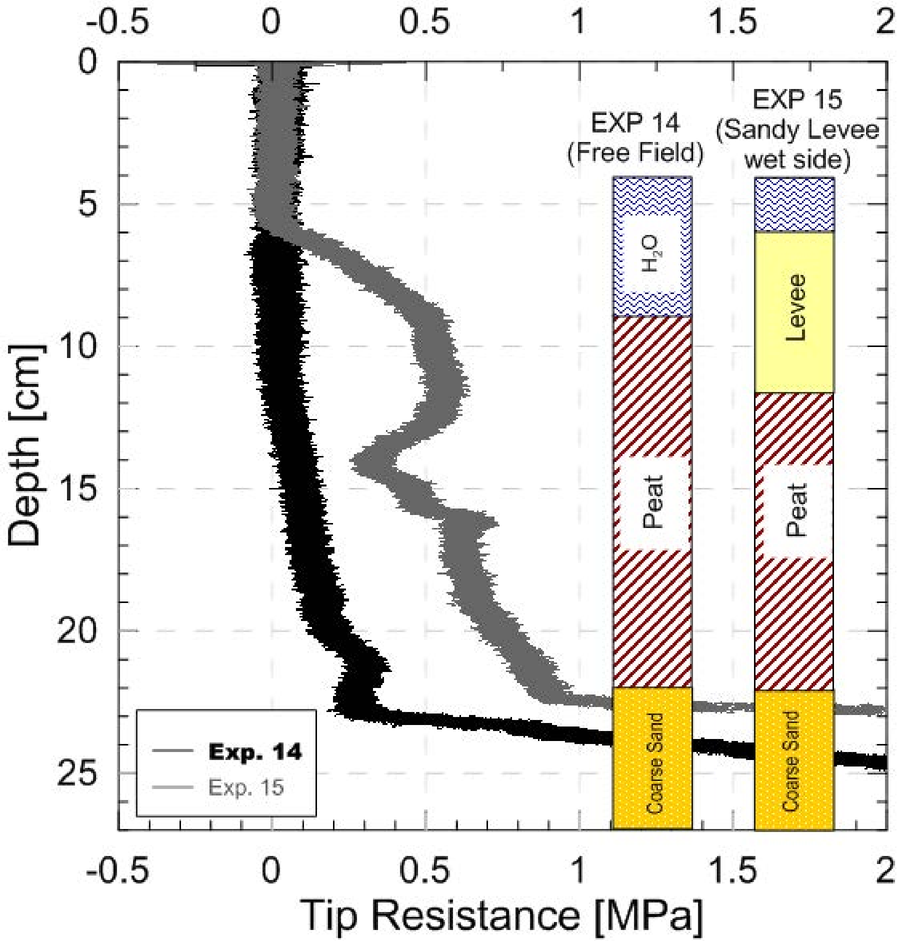

-0.5
0
0.5
1
1.5
2
Depth [cm]
Tip Resistance [MPa]
EXP 14 (Free Field)
EXP 15 (Sandy Levee wet side)
H_2O
Levee
Peat
Peat
Coarse Sand
Coarse Sand
Exp. 14
Exp. 15

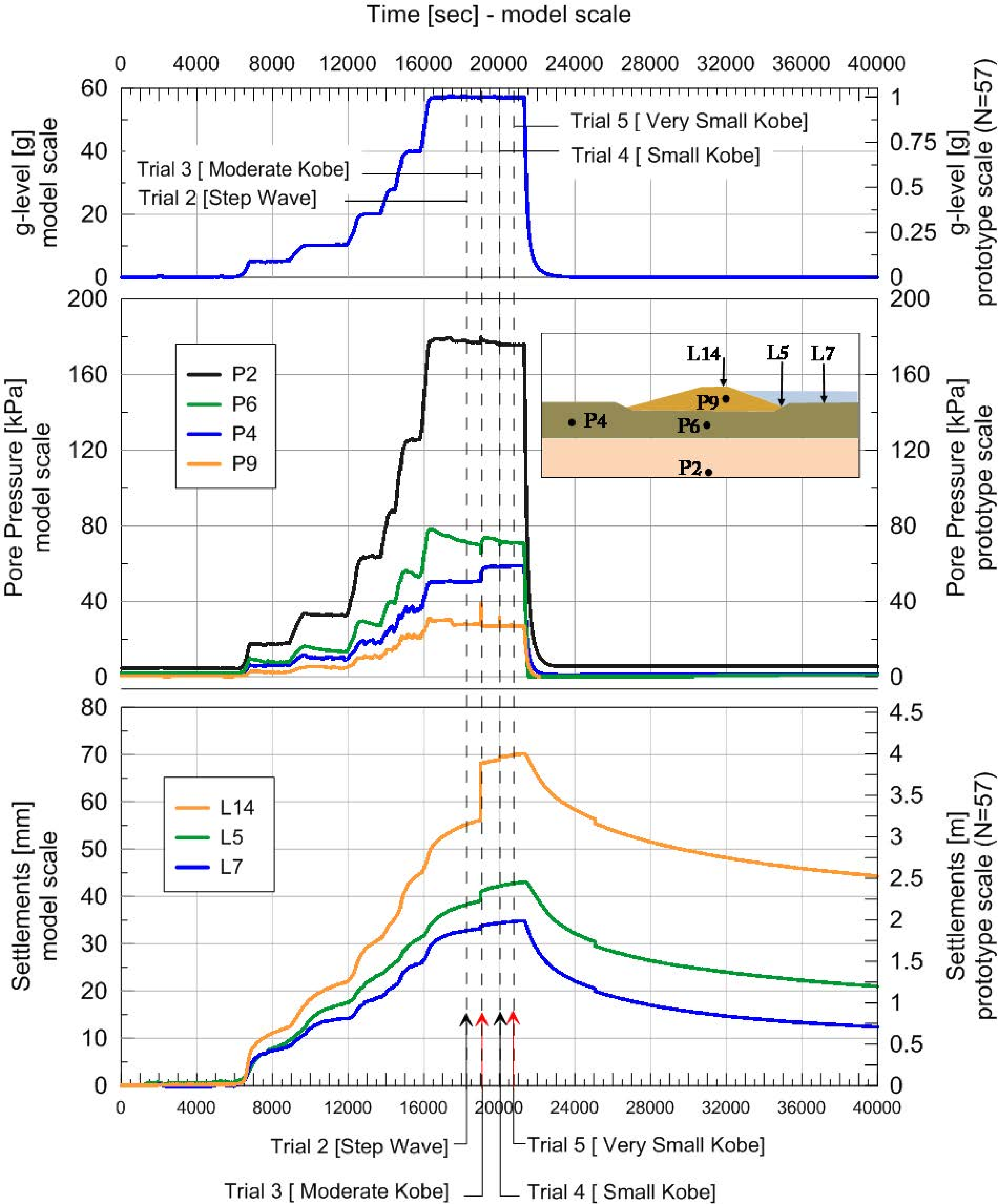

Time [sec] - model scale
g-level [g] model scale
g-level [g] prototype scale (N=57)
Trial 5 [Very Small Kobe]
Trial 4 [Small Kobe]
Trial 3 [Moderate Kobe]
Trial 2 [Step Wave]
Pore Pressure [kPa] model scale
Pore Pressure [kPa] prototype scale
P2
P6
P4
P9
L14
L5
L7
Settlements [mm] model scale
Settlements [m] prototype scale (N=57)

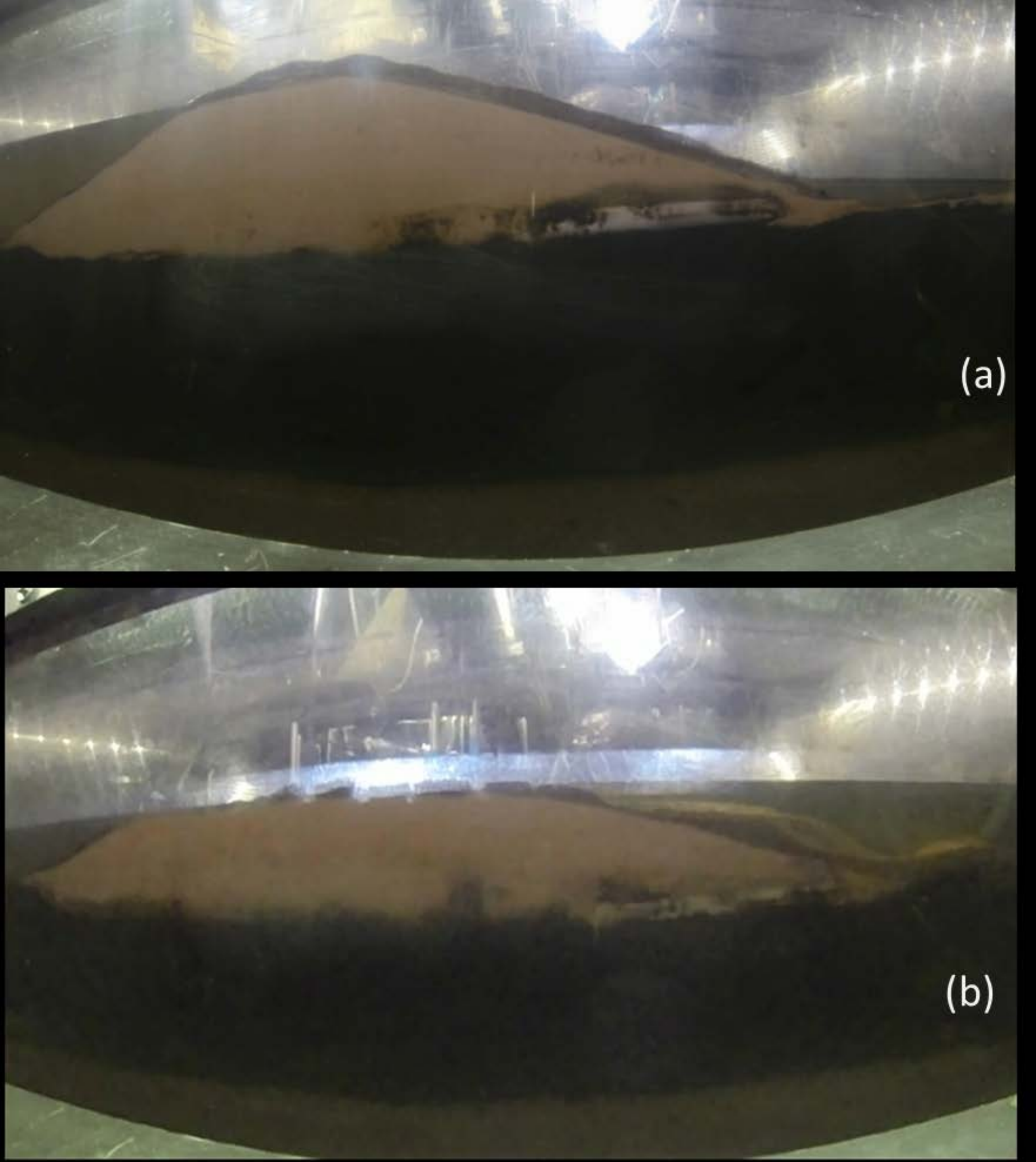
(a)
(b)

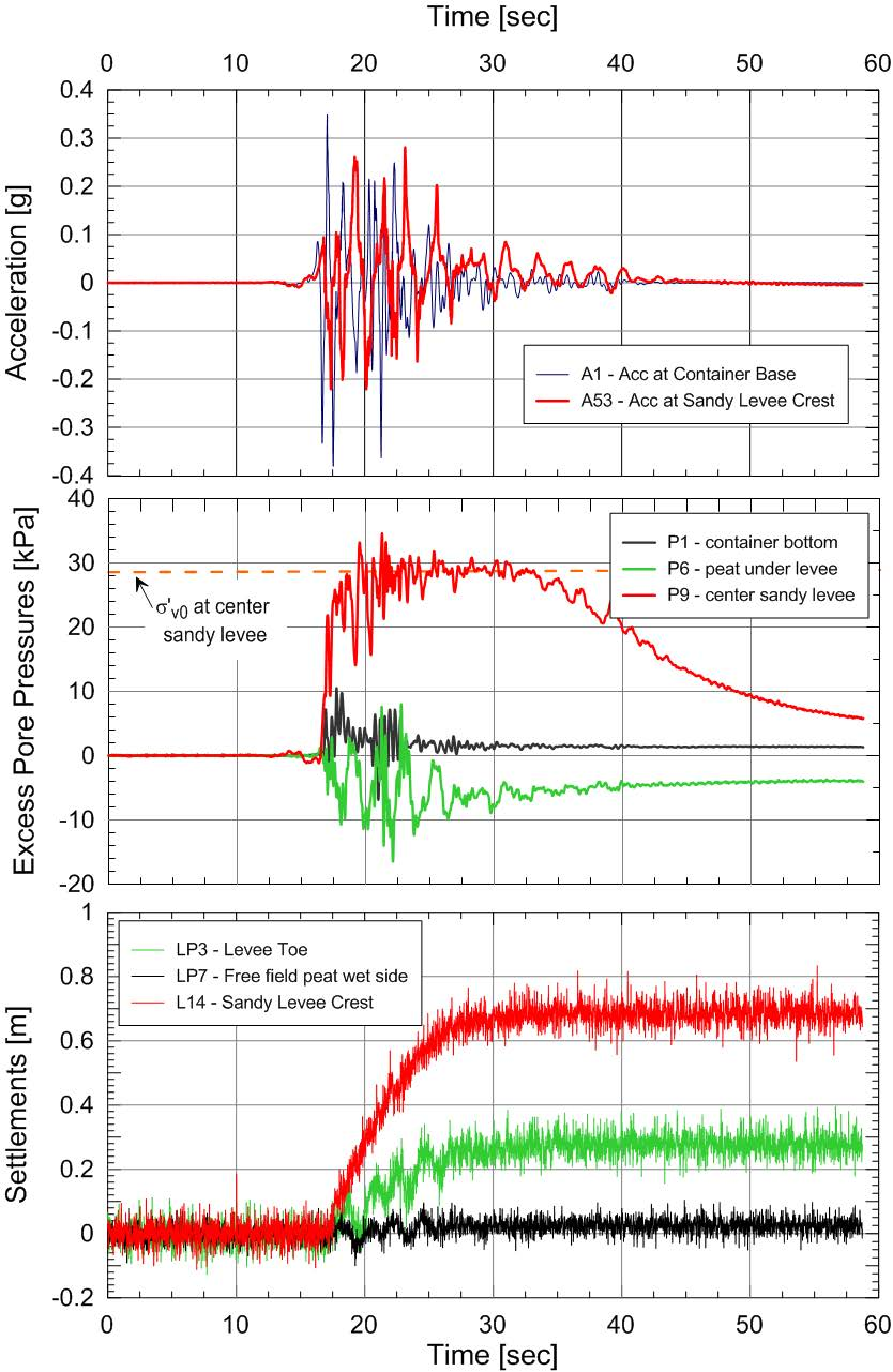
Time [sec]
Acceleration [g]
A1 - Acc at Container Base
A53 - Acc at Sandy Levee Crest
Excess Pore Pressures [kPa]
σ'v0 at center sandy levee
P1 - container bottom
P6 - peat under levee
P9 - center sandy levee
Settlements [m]
LP3 - Levee Toe
LP7 - Free field peat wet side
L14 - Sandy Levee Crest
Time [sec]